

Supporting Information

Shahmoon et al. 10.1073/pnas.1401346111

SI Text

Dispersion Energy Mediated by the Transverse Electric and Transverse Magnetic Modes of a Coaxial Line

In the main text we analyzed the dispersion energy, namely, van der Waals (vdW) or Casimir interaction energy, between dipoles that are coupled via the transverse electromagnetic (TEM) mode of a transmission line (TL). Here we outline the calculation of the contribution of higher-order transverse modes and show that (i) their contribution is negligible with respect to that of the TEM mode for $z > a$, where z is the interdipolar distance and a is the typical separation between the two conductors that compose the TL, and (ii) in the limit $z \ll a$ their contribution sums up to be that of free space.

In the following we demonstrate these results for a coaxial line (Fig. 1A in the main text), where most calculations can be performed analytically.

Dispersion Energy Mediated by Modes with a Cutoff. In ref. 1, the dispersion energy mediated by the modes of a metallic waveguide is analyzed, and a formalism for a general case where the typical scale for confinement a that is much smaller than the typical dipole transition wavelength λ_c is developed. We follow a similar approach.

We consider modes with normalized mode functions and dispersion relation

$$\mathbf{u}_{lmk}^\mu(\mathbf{r}) = \frac{1}{\sqrt{L}} e^{ikz} \mathbf{E}_{lmk}^\mu(x, y), \quad \omega_{lmk}^\mu = c \sqrt{(k_{lm}^\mu)^2 + k^2}, \quad [\text{S1}]$$

respectively. Here k is the wavenumber at the propagation axis z with quantization length L , μ is the index of the polarization, and l and m are indexes of the transverse mode whose dependence on the transverse coordinates is described by $\mathbf{E}_{lmk}^\mu(x, y)$ and its cutoff frequency is ck_{lm}^μ . When the confinement is tight, namely for $a \ll \lambda_n \forall n$, where we recall the excited states with energies $E_n = \hbar 2\pi c / \lambda_n$, and because typically $k_{lm}^\mu \geq \pi/a$ (also in the coaxial line, see below), then $\omega_{lmk}^\mu \gg E_n / \hbar \forall n$, and the dispersion energy, Eq. 3 in the main text, can be approximated as (1)

$$U \approx -\frac{1}{(2\pi\epsilon)^2} \sum_{n_1, n_2} \sum_{ijpq} \frac{d_{n_1 i} d_{n_1 j} d_{n_2 p} d_{n_2 q}}{E_{n_1} + E_{n_2}} F_{n_2 ij} F_{n_1 pq},$$

$$F_{nij} = \sum_{\mu lm} F_{lm, nij}^\mu, \quad [\text{S2}]$$

$$F_{lm, nij}^\mu = \int_{-\infty}^{\infty} dk \frac{\omega_{lmk}^\mu}{\omega_{lmk}^\mu + E_n / \hbar} \mathbf{E}_{lmk, i}^\mu(x_2, y_2) \mathbf{E}_{lmk, j}^{\mu*}(x_1, y_1) e^{ikz}.$$

The indices i, j, p , and q run over the projections of the vectors \mathbf{d}_n and $\mathbf{E}_{lmk}^\mu(x, y)$ onto the x, y, z directions, e.g., $d_{nx} = \mathbf{d}_n \cdot \mathbf{e}_x$.

Transverse Modes of a Coaxial Transmission Line. Apart from the TEM mode, the coaxial TLs possess transverse electric (TE) and transverse magnetic (TM) modes. In ref. 2 their mode functions are found, and we normalize them such that $\int_a^b d\rho \int_0^{2\pi} d\phi \mathbf{E}_{lmk}^{\mu*}(\rho, \phi) \cdot \mathbf{E}_{lmk}^\mu(\rho, \phi) = 1$, with the polar coordinates being $\rho = \sqrt{x^2 + y^2}$, $\phi = \arctan(y/x)$. Their dispersion relations are those from Eq. S1 above, with $\mu = \text{TE, TM}$. The cutoff

wavenumbers are determined by the transcendental equations (2)

$$\begin{aligned} J'_l(k_l^{\text{TE}} a) Y'_l(k_l^{\text{TE}} b) - Y'_l(k_l^{\text{TE}} a) J'_l(k_l^{\text{TE}} b) &= 0, \\ J_l(k_l^{\text{TE}} a) Y_l(k_l^{\text{TE}} b) - Y_l(k_l^{\text{TE}} a) J_l(k_l^{\text{TE}} b) &= 0, \end{aligned} \quad [\text{S3}]$$

for TE and TM, respectively. Here $J_l(x)$ and $Y_l(x)$ are the Bessel functions of order l , of the first and the second kind, respectively, and $J'_l(x)$, $Y'_l(x)$ are their derivatives. For each $\mu = \text{TE, TM}$, and l , the infinite solutions of the transcendental equation for the k_l^μ are ordered by the index m , and hence k_{lm}^μ .

The corresponding normalized mode functions are given by

$$\begin{aligned} \mathbf{E}_{lmk}^{\text{TE}}(\rho, \phi) &= D_{lm}^{\text{TE}} \left([Y'_l(k_{lm}^{\text{TE}} a) J'_l(k_{lm}^{\text{TE}} \rho) \right. \\ &\quad \left. - J'_l(k_{lm}^{\text{TE}} a) Y'_l(k_{lm}^{\text{TE}} \rho)] \cos(l\phi) \mathbf{e}_\phi \right. \\ &\quad \left. + \frac{l}{k_{lm}^{\text{TE}} \rho} [Y'_l(k_{lm}^{\text{TE}} a) J_l(k_{lm}^{\text{TE}} \rho) \right. \\ &\quad \left. - J'_l(k_{lm}^{\text{TE}} a) Y_l(k_{lm}^{\text{TE}} \rho)] \sin(l\phi) \mathbf{e}_\rho \right) \end{aligned} \quad [\text{S4}]$$

$$\mathbf{E}_{lmk}^{\text{TM}}(\rho, \phi) = D_{lmk}^{\text{TM}} \left(k_{lm}^{\text{TM}} \tilde{E}_{lm, z}^{\text{TM}} \mathbf{e}_z + ik \tilde{E}_{lm, x}^{\text{TM}} \mathbf{e}_x + ik \tilde{E}_{lm, y}^{\text{TM}} \mathbf{e}_y \right),$$

with

$$\begin{aligned} \tilde{E}_{lm, z}^{\text{TM}}(\rho, \phi) &= [Y_l(k_{lm}^{\text{TM}} a) J_l(k_{lm}^{\text{TM}} \rho) \\ &\quad - J_l(k_{lm}^{\text{TM}} a) Y_l(k_{lm}^{\text{TM}} \rho)] \cos(l\phi), \\ \tilde{E}_{lm, x}^{\text{TM}}(\rho, \phi) &= [Y_l(k_{lm}^{\text{TM}} a) J'_l(k_{lm}^{\text{TM}} \rho) \\ &\quad - J_l(k_{lm}^{\text{TM}} a) Y'_l(k_{lm}^{\text{TM}} \rho)] \cos(l\phi) \cos(\phi) \\ &\quad - \frac{l}{k_{lm}^{\text{TM}} \rho} [Y_l(k_{lm}^{\text{TM}} a) J_l(k_{lm}^{\text{TM}} \rho) \\ &\quad - J_l(k_{lm}^{\text{TM}} a) Y_l(k_{lm}^{\text{TM}} \rho)] \sin(l\phi) \sin(\phi), \\ \tilde{E}_{lm, y}^{\text{TM}}(\rho, \phi) &= -[Y_l(k_{lm}^{\text{TM}} a) J'_l(k_{lm}^{\text{TM}} \rho) \\ &\quad - J_l(k_{lm}^{\text{TM}} a) Y'_l(k_{lm}^{\text{TM}} \rho)] \cos(l\phi) \sin(\phi) \\ &\quad - \frac{l}{k_{lm}^{\text{TM}} \rho} [Y_l(k_{lm}^{\text{TM}} a) J_l(k_{lm}^{\text{TM}} \rho) \\ &\quad - J_l(k_{lm}^{\text{TM}} a) Y_l(k_{lm}^{\text{TM}} \rho)] \sin(l\phi) \cos(\phi). \end{aligned} \quad [\text{S5}]$$

The normalization factors D_{lm}^{TE} and D_{lmk}^{TM} in Eq. S4 depend on a and b ; however, only D_{lmk}^{TM} depends on the wavenumber k . Hence, as is seen below, the exact expression for D_{lm}^{TE} is not needed for our calculations here, whereas D_{lmk}^{TM} is given by

$$\begin{aligned} D_{lmk}^{\text{TM}} &= \frac{1}{\sqrt{\pi}} \left(Y_l^2(k_{lm}^{\text{TM}} a) \left[\tilde{J}_{l, lm} + \left(\frac{k}{k_{lm}^{\text{TM}}} \right)^2 I'_{l, lm} + l^2 \left(\frac{k}{k_{lm}^{\text{TM}}} \right)^2 I_{l, lm} \right] \right. \\ &\quad \left. - 2Y_l(k_{lm}^{\text{TM}} a) J_l(k_{lm}^{\text{TM}} a) \left[\tilde{J}'_{Y, lm} + \left(\frac{k}{k_{lm}^{\text{TM}}} \right)^2 I'_{Y, lm} + l^2 \left(\frac{k}{k_{lm}^{\text{TM}}} \right)^2 I_{Y, lm} \right] \right) \end{aligned}$$

$$\begin{aligned}
& + J_l^2(k_{lm}^{\text{TM}} a) \left[\tilde{I}_{Ylm} + \left(\frac{k}{k_{lm}^{\text{TM}}} \right)^2 I'_{Ylm} + l^2 \left(\frac{k}{k_{lm}^{\text{TM}}} \right)^2 I_{Ylm} \right]; \quad \text{for } l > 0, \\
D_{0mk}^{\text{TM}} & = \frac{2}{\sqrt{\pi}} \left(Y_l^2(k_{lm}^{\text{TM}} a) \left[\tilde{I}_{Jlm} + \left(\frac{k}{k_{lm}^{\text{TM}}} \right)^2 I'_{Jlm} \right] \right. \\
& \quad \left. - 2Y_l(k_{lm}^{\text{TM}} a) J_l(k_{lm}^{\text{TM}} a) \left[\tilde{I}_{YJlm} + \left(\frac{k}{k_{lm}^{\text{TM}}} \right)^2 I'_{YJlm} \right] \right. \\
& \quad \left. + J_l^2(k_{lm}^{\text{TM}} a) \left[\tilde{I}_{Ylm} + \left(\frac{k}{k_{lm}^{\text{TM}}} \right)^2 I'_{Ylm} \right] \right); \quad \text{for } l = 0,
\end{aligned} \tag{S6}$$

where

$$\begin{aligned}
\tilde{I}_{Jlm} & = \int_{k_{lm}^{\text{TM}a}^{k_{lm}^{\text{TM}b}} dx x J_l^2(x), & \tilde{I}_{Ylm} & = \int_{k_{lm}^{\text{TM}a}^{k_{lm}^{\text{TM}b}} dx x Y_l^2(x), \\
\tilde{I}_{YJlm} & = \int_{k_{lm}^{\text{TM}a}^{k_{lm}^{\text{TM}b}} dx x Y_l(x) J_l(x), & I'_{Jlm} & = \int_{k_{lm}^{\text{TM}a}^{k_{lm}^{\text{TM}b}} dx x J_l'^2(x), \\
I'_{Ylm} & = \int_{k_{lm}^{\text{TM}a}^{k_{lm}^{\text{TM}b}} dx x Y_l'^2(x), & I'_{YJlm} & = \int_{k_{lm}^{\text{TM}a}^{k_{lm}^{\text{TM}b}} dx x Y_l'(x) J_l'(x), \\
I_{Jlm} & = \int_{k_{lm}^{\text{TM}a}^{k_{lm}^{\text{TM}b}} dx \frac{1}{x} J_l'^2(x), & I_{Ylm} & = \int_{k_{lm}^{\text{TM}a}^{k_{lm}^{\text{TM}b}} dx \frac{1}{x} Y_l'^2(x), \\
I_{YJlm} & = \int_{k_{lm}^{\text{TM}a}^{k_{lm}^{\text{TM}b}} dx \frac{1}{x} Y_l'(x) J_l'(x).
\end{aligned} \tag{S7}$$

Dispersion Energy: Results. TE modes. The dispersion energy is obtained by inserting $\mathbf{E}_{lm}^{\text{TE}}$ from Eq. S4 into Eq. S2 for the energy U . We note that for TE modes $\mathbf{E}_{lm}^{\text{TE}}$ does not depend on k , so it can be taken out of the integral for $F_{lm,nij}^{\text{TE}}$. This is also the case for TE modes in a metallic waveguide, where we get (1)

$$F_{lm,nij}^{\text{TE}} \approx -E_{lm,i}^{\text{TE}}(\rho_2, \phi) E_{lm,j}^{\text{TE}*}(\rho_1, \phi_1) K_0(k_{lm}^{\text{TE}} z), \tag{S8}$$

$K_0(x)$ being the zeroth-order modified Bessel function.

TM modes. For TM modes, we first approximate the integrand in $F_{lm,nij}^{\text{TM}}$ by $\omega_{lmk}^\mu / (\omega_{lmk}^\mu + E_n/\hbar) \approx 1$, recalling that $\omega_{lmk}^\mu \gg E_n/\hbar$. Then, the resulting integrations for $F_{lm,nij}^{\text{TM}}$ are similar to those encountered in ref. 1 for the metallic-waveguide case, and we find

$$F_{lm,nzz}^{\text{TM}} \approx \frac{|\tilde{E}_{lm,z}^{\text{TM}}|^2}{\tilde{D}_{lm} D_{lm}} (k_{lm}^{\text{TM}})^3 e^{-\frac{\tilde{D}_{lm} k_{lm}^{\text{TM}} z}{D_{lm}}},$$

$$\begin{aligned}
F_{lm,nij}^{\text{TM}} & \approx -\frac{\tilde{E}_{lm,i}^{\text{TM}} \tilde{E}_{lm,j}^{\text{TM}*} \tilde{D}_{lm}}{D_{lm}^3} (k_{lm}^{\text{TM}})^3 e^{-\frac{\tilde{D}_{lm} k_{lm}^{\text{TM}} z}{D_{lm}}}; \quad \text{for } i=x,y; j=x,y, \\
F_{lm,nzi}^{\text{TM}} & \approx -\frac{\tilde{E}_{lm,i}^{\text{TM}} \tilde{E}_{lm,j}^{\text{TM}*}}{D_{lm}^2} (k_{lm}^{\text{TM}})^3 e^{-\frac{\tilde{D}_{lm} k_{lm}^{\text{TM}} z}{D_{lm}}}; \quad \text{for } i=x,y,
\end{aligned} \tag{S9}$$

with

$$\begin{aligned}
\tilde{D}_{lm}^2 & = Y_l^2(k_{lm}^{\text{TM}} a) \tilde{I}_{Jlm} - 2Y_l(k_{lm}^{\text{TM}} a) J_l(k_{lm}^{\text{TM}} a) \tilde{I}_{YJlm} + J_l^2(k_{lm}^{\text{TM}} a) \tilde{I}_{Ylm}, \\
D_{lm}^2 & = Y_l^2(k_{lm}^{\text{TM}} a) [I'_{Jlm} + l^2 I_{Jlm}] \\
& \quad - 2Y_l(k_{lm}^{\text{TM}} a) J_l(k_{lm}^{\text{TM}} a) [I'_{Ylm} + l^2 I_{Ylm}] \\
& \quad + J_l^2(k_{lm}^{\text{TM}} a) [I_{YJlm} + l^2 I_{Ylm}].
\end{aligned} \tag{S10}$$

Retarded Limit: $z \gg a$. Let us assume $b = 2a$ for simplicity, such that a sets the scale for the confinement. The cutoff wave-numbers k_{lm}^μ exist due to the confinement a , and hence we expect them to satisfy $k_{lm}^\mu \geq \pi/a$. This is verified by solving numerically the transcendental Eqs. S3, where we find, e.g., $k_{11}^{\text{TM}} a = 3.1966$ and $k_{1,500,1,500}^{\text{TM}} a = 2,992$. For TM modes we further verify that $\frac{\tilde{D}_{lm}}{D_{lm}} k_{lm}^{\text{TM}} a \geq 1$ such that at the retarded limit, $z \gg a$, $F_{lm,nij}^{\text{TM}}$ from Eq. S9 are all very small due to the exponential decay. Moreover, for TE modes we can take the asymptotic limit $K_0(x) \approx \sqrt{\pi/(2x)} e^{-x}$, obtaining $F_{lm,nij}^{\text{TE}} \propto \sqrt{1/ze^{-k_{lm}^{\text{TE}} z}}$. This leads to the conclusion that the contribution of TE and TM modes to the dispersion energy in the retarded regime is exponentially decaying and negligible with respect to that of the TEM mode.

Van der Waals Limit: $z \ll a$. TE modes. Using exactly the same arguments as in the metal-waveguide case, based on the approximation $K_0(x) \sim \ln(x) + \text{const.}$ for small x , we can show that the contribution of the TE modes to the energy in the $z \ll a$ limit scales as in ref. 1, $(\ln z/z)^2$. This scaling is more weakly divergent than the vdW limit in free space, which scales as $1/z^6$; hence TE modes cannot explain how the free-space result is restored at short distances and is not dominant in this regime.

TM modes. When the dipoles are placed at the center, between the two conductors at $\rho = 1.5a$, and are close enough such that $z \ll a$, they do not “sense” the structure of the coaxial waveguide and their interaction energy is expected to be that of free space. Our previous conclusion, that TE modes do not give rise to such interaction, suggests that the TM modes are the dominant interaction mediators in the vdW, short-range, regime and that their contributions sum up to give the free-space result. This is shown analytically for the TM modes of a metallic waveguide in ref. 1. Here, k_{lm}^{TM} can be calculated only numerically from Eq. S3, and we demonstrate it, e.g., for the case where the dipoles can be polarized only in the z direction ($d_{ni} = d_{nz} \delta_{iz}$). The vdW energy from Eq. S2 then becomes

$$U \approx -\frac{1}{(2\pi\epsilon)^2} \sum_{n_1, n_2} \frac{d_{n_2 z}^2 d_{n_1 z}^2}{E_{n_1} + E_{n_2}} F_{zz}^2, \quad F_{zz} \approx \sum_{lm} F_{lm,nij}^{\text{TM}}, \tag{S11}$$

where $F_{lm,nzz}^{\text{TM}}$ is the one from Eq. S9. In Fig. S1 we present the numerical summation of $a^3 F_{zz}$ as a function of z , for $\rho = 1.5a$ and up to $l = 800, m = 1,500$. An excellent agreement with $F_{zz} = 1/z^3$

is obtained, which gives exactly the vdW energy in free space for this case (3).

Imperfections

Inhomogeneity of the Dipolar Transition Energies. In the main text we mentioned the possibility of inhomogeneity of the parameters of the dipolar transition in artificial systems such as superconducting transmons. This means that fluctuations of a few percent about the parameters E_n and \mathbf{d}_n of a transition $|g\rangle \rightarrow |n\rangle$ may exist due to inaccuracy in the circuit production process. Whereas the spatial structure of the vacuum interaction energy between two general dipoles $U(z)$ (Eqs. 11–13 in the main text) does not depend on these dipole parameters, its numerical value, including all prefactors, does. Therefore, depending on the amount of inaccuracy with respect to the interaction energy $U(z)$ one wishes to measure, the (exact) evaluation of $U(z)$ may require one to first measure the dipolar parameters of each transmon separately, when it is decoupled from the other transmon. Because the transmons are coupled only via the TL, the latter requirement amounts to the ability to decouple a transmon from the TL. This may be achieved by, e.g., externally controlling the capacitive coupling of the transmon to the TL (4).

Single-Dipole Energy Shifts Induced by TL Conductors. For atomic and molecular dipoles, single-dipole energy shifts and hence inhomogeneities may exist due to the (vacuum-mediated) interaction of each dipole with the conductors that compose the TL. These energy shifts can be viewed as the modified Lamb shift

experienced by a dipole due to the electromagnetic vacuum modes near a metal. For dipoles as small as atoms, we estimate this dipole–metal interaction energy by the so-called Casimir–Polder or vdW potential of a polarizable particle near a surface (5, 6):

$$\delta E = \frac{\hbar}{4\pi l^3} \int_0^\infty d\omega \text{Im} \left\{ \frac{1 - \epsilon(\omega)}{1 + \epsilon(\omega)} \alpha(\omega) \right\}. \quad [\text{S12}]$$

Here l is the distance between the dipole and the surface, $\epsilon(\omega)$ is the bulk dielectric response of the surface, and $\alpha(\omega)$ is the particle polarizability. This expression is correct in the nonretarded limit, where the distance l , typically on the order of $1 \mu\text{m}$ in the circuit quantum electrodynamics (QED) case, is much smaller than the typical/dominant wavelength of the dipolar transition. Considering the complex dielectric response of TL conductors $\epsilon(\omega)$, the perfect lossless conductor limit is given by $\text{Re}\{\epsilon\} \rightarrow -\infty$ and $\text{Im}\{\epsilon\} = 0$. Nevertheless, Eq. S12 yields a dispersive (real) energy shift regardless of the fact that in practice ϵ may have an imaginary part (losses). Indeed, because the system as a whole is in its (unperturbed) ground state (vacuum for the photons and ground state for dipoles), and the only excitations it exhibits are virtual, irreversible effects due to losses are not expected to play a role. The effect of losses in either the conductors or the dipoles is manifest in Eq. S12 by the frequency dependence of ϵ or α , respectively: The Kramers–Kronig relations determine their real and imaginary parts.

1. Shahmoon E, Kurizki G (2013) Dispersion forces inside metallic waveguides. *Phys Rev A* 87(6):062105.
2. Pozar DM (2005) *Microwave Engineering* (Wiley, New York).
3. Craig DP, Thirunamachandran T (1984) *Molecular Quantum Electrodynamics* (Academic, London).
4. Koch J, et al. (2007) Charge-insensitive qubit design derived from the Cooper pair box. *Phys Rev A* 76(4):042319.

5. Barash YS, Ginzburg VL (1984) Some problems in the theory of van der Waals forces. *Sov Phys Usp* 27(7):467.
6. Intravaia F, Henkel C, Antezza M (2011) Fluctuation-induced forces between atoms and surfaces: The Casimir-Polder interaction. *Casimir Physics, Lecture Notes in Physics* (Springer, Berlin), Vol 834, pp 345–391.

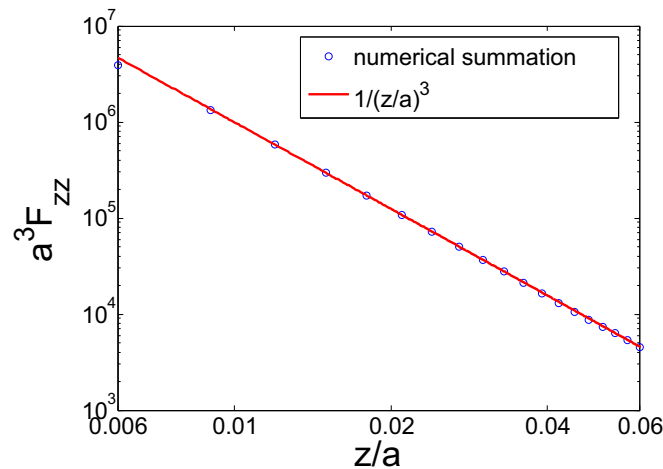


Fig. S1. Evaluation of the sum F_{zz} in Eq. S11: log–log plot of the result of the direct numerical summation compared with the curve $1/(z/a)^3$.